

BEAM TRACKING FOR J-PARC 3 GEV RCS INJECTION

M. J. Shirakata, H. Fujimori, KEK, Tsukuba, Japan
 Y. Irie, JAEA, Tokai, Japan

Abstract

In the J-PARC 3 GeV RCS injection system, the orbit-bump magnets of large-bore are located closely each other, and the incoming beam passes through the non-linear field region of the ring quadrupole magnet. Beam behavior under these conditions is analysed by means of the Runge-Kutta method in the three dimensional magnetic field distribution. The charge exchange foil is inserted between the bump magnets. Orbit of the stripped electrons from the foil is also investigated.

BEAM INJECTION TO THE J-PARC RCS

The J-PARC accelerator complex shown in Fig. 1 consists of LINAC, Rapid Cycling Synchrotron (RCS) and main ring. The RCS ring is designed to have very large aperture more than 400π mm mrad for high intensity proton beam and a beam painting upto 216π mm mrad is planned for the injection scheme. A schematic view of the injection section of the RCS is shown in Fig. 2. The RCS injection system consists of four shift-bump magnets, four paint-bump magnets and three electron stripper. The electron stripper for the incoming H^- beam is made with a carbon foil of $300 \mu\text{m}$ thick. The primary carbon foil is used for the beam injection into the ring orbit. The 2nd and 3rd carbon foils are used for the beam dump of unstripped H^0 and H^- passed through the primary foil. The shift-bump magnets form an injection-bump orbit of 90 mm outside at the primary foil. The paint-bump magnets sweep the orbit at the foil with the range corresponding to 216π mm mrad beam emittance for the horizontal plane. For the vertical plane, a steering magnet is utilized for the vertical painting and the painting size is the same as the horizontal one.

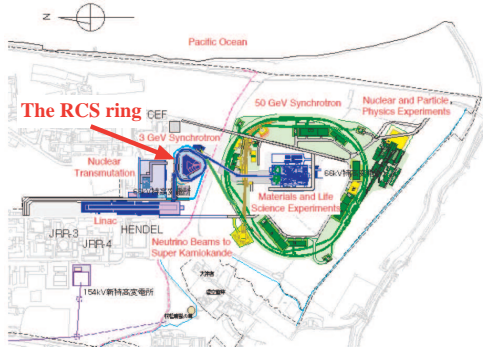


Figure 1: Overview of the J-PARC site.

On the simulation of the beam injection, there are six topics should be taken in to account as follows:

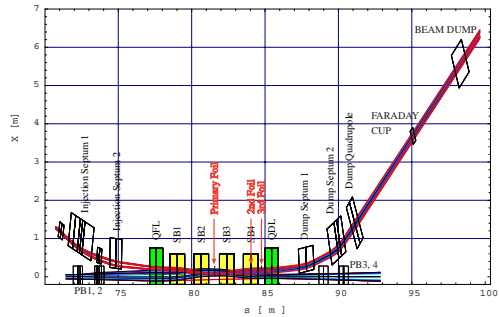


Figure 2: A schematic view of the RCS injection section.

- Passage through non-linear field
- Passage through interfering field
- Effective beam emittance under the pulse-to pulse field fluctuations
- Mismatched injection
- Large beam size in the dump line
- Stripped electrons

Then, the targets of the simulation are summarized as follows:

- Influence of the interfering and non-linear fields
- Hitting rate of the primary stripping foil
- Trajectory of stripped electrons

As shown in Fig. 3, the incoming beam passes far from the linear field region of the ring quadrupole QFL. The field gradient decreases by about 27% in the corresponding beam orbit. The beam distribution in phase space is deformed according to the non-linear field from the QFL.

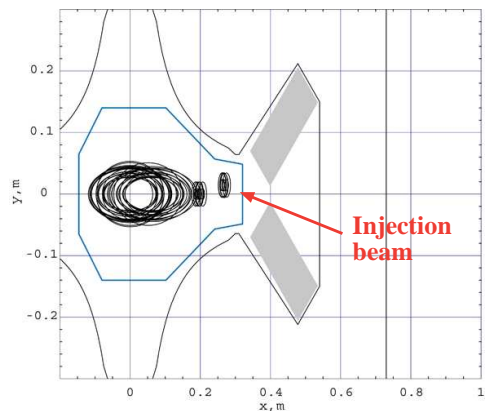


Figure 3: The incoming beam position at the QFL.

Ring quadrupoles QFL and QDL and shift-bump magnets are installed in crowded and their iron cores interfere

neighbouring magnetic fields each other. In order to treat the complicated magnetic field, the distributed magnetic field dataset, which consists of distributed three dimensional vectors defined on the rectangular lattice structure as shown in Fig. 4, and the whole system calculation method are adopted [1][2][3]. The magnetic fields are calculated by OPERA-3D for the shift-bump area which includes two ring quadrupoles, paint-bump areas, injection septum areas and dump septum areas.

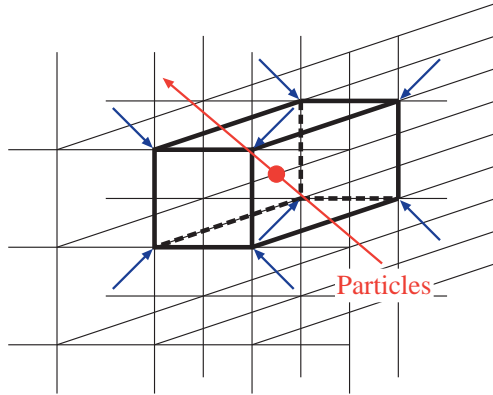


Figure 4: A lattice structure of the magnetic field definition. The magnetic field at the particle position is interpolated from eight vectors around the particle.

Though the calculated field data is generated with the design currents, the field integrations along the design beam orbit $B_y l$ of each magnet components are different from the required values because of the field interferences. As shown in Fig. 5, the normalization by using the design $B_y l$ is necessary in order to represent the design beam orbit. The normalization for the quadrupoles is also necessary in order to correct the tune-shift.

The incoming H^- beam is horizontally perturbed by the time-varying field during passage to the primary carbon foil. The stabilities/precisions of the relevant fields are assumed in Table 1. On the other hand, vertical errors are

Table 1: Perturbations in horizontal phase space

Source	Contribution
Pulsed injection septum 1&2	$\leq \pm 0.5 \%$
Ring quadrupole (QFL)	$\leq \pm 0.2 \%$
Shift bumps 1-4 in series	$\leq \pm 1.0 \%$

taken at the entrance of the injection line as:

- $y_0 = 20.879(1 \pm 0.05)$ mm, $\Delta y_0 = \pm 1.04$ mm
- $y'_0 = -0.9055(1 \pm 0.05)$ mrad, $\Delta y'_0 = \pm 0.045$ mrad

The effective emittance is evaluated as $\epsilon_x = 11.3\pi$ and $\epsilon_y = 8.9\pi$ mm mrad as shown in Fig. 6 with the parameters of the linac beam at the foil in the worst case, respectively. In addition, the twiss parameters of incoming H^- beam are not matched to the ring optics. The ring bump orbit and the

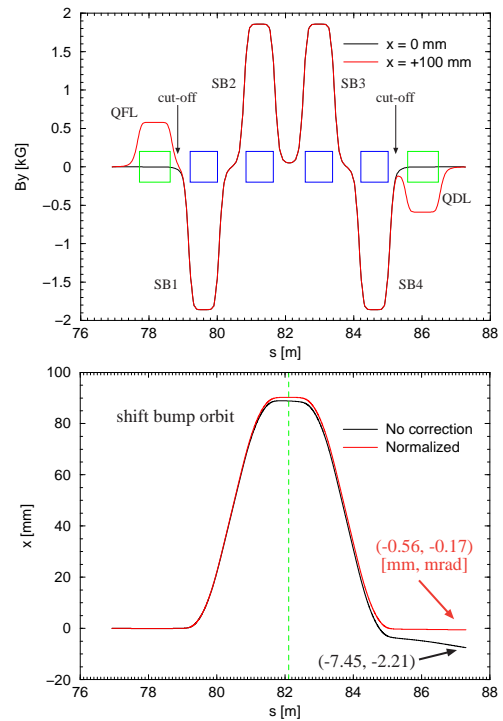


Figure 5: Calculated magnetic field and the corresponding central beam orbit.

painting range are changed in order to accommodate the effective emittance within the original painting area.

RESULTS

The particle tracking is executed by TRACY-II [4] with the complicated magnetic field datasets using the Runge-Kutta integrator. The central orbit of the incoming beam is examined for the dumped beam as shown in Fig. 7. Unstripped component of the incoming H^- beam is transferred to the beam dump. The particle distributions in phase space are checked about the field quality of dump septum magnets and aperture margins in the dump line.

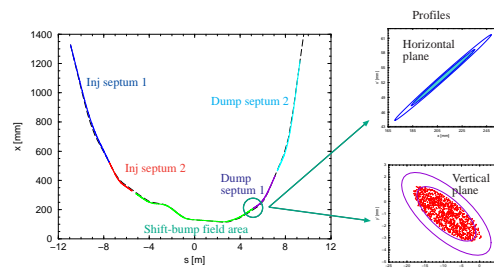


Figure 7: Inspection of the dump line.

Painting process is simulated without space charge force. Beam footprints at the end of the injection period are shown in Fig. 8. No significant dilutions nor emittance growth can be observed. However, hitting probability of the primary

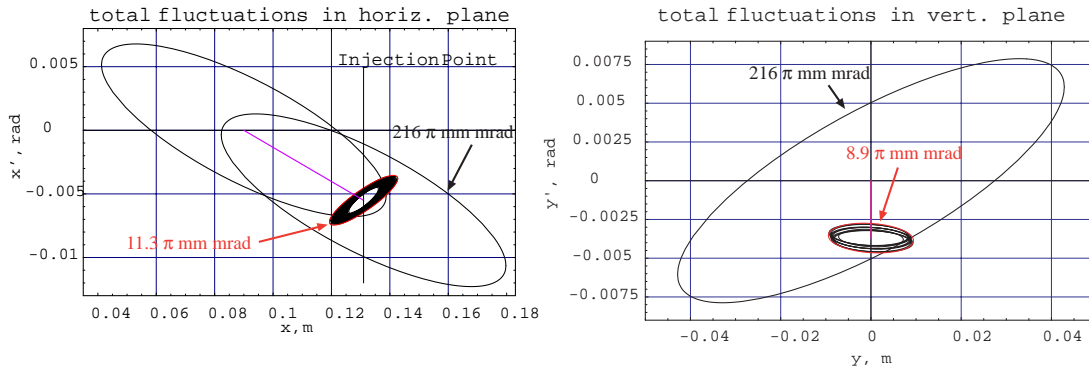


Figure 6: Estimated effective beam emittances of the incoming beam.

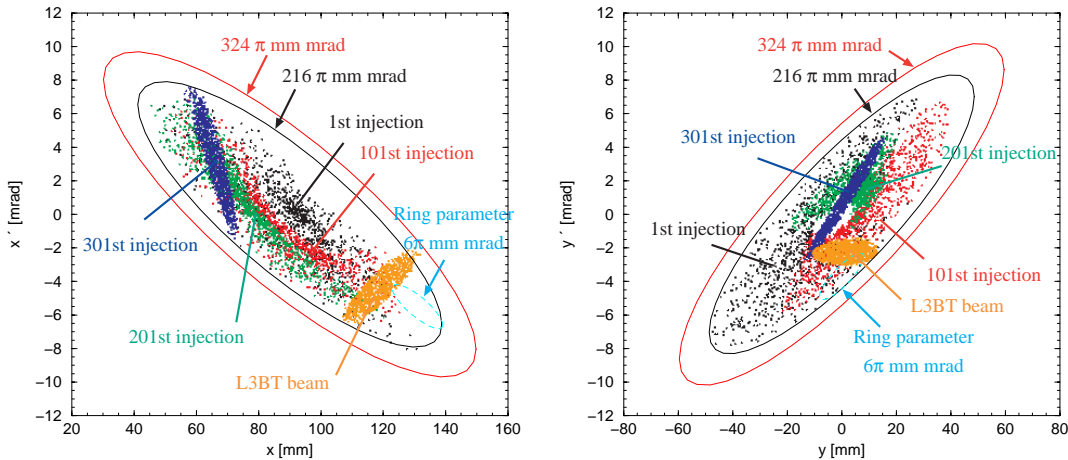


Figure 8: Footprints of the circulating proton bunch.

carbon foil by the circulating beam increases with the modified painting range.

The stripped electron tracking is needed for the design of an electron catcher. Electrons return toward the foil frame and diffuse vertically due to the B_z component from SB2 and SB3 as shown in Fig. 9. In this calculation, the incoming beam emittance is assumed slightly wider.

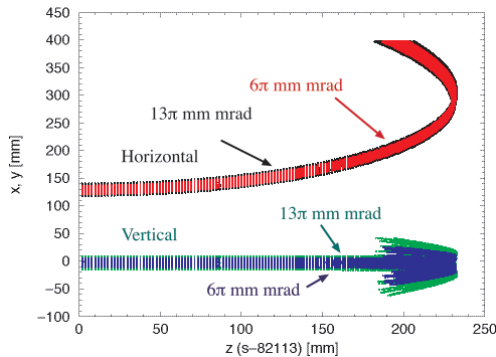


Figure 9: Trajectories of the stripped electrons.

The simulation of the RCS injection is summarized as follows:

- Beam injection process was simulated with the distributed magnetic field vectors.
- Beam-dump scheme of unstripped component is expected to work well.
- Field interference causes the orbit distortion and tune shift but no emittance growth.
- Increase of foil hits by the circulating beam requires further analysis of loss distributions, foil temperature and injection parameter optimization.
- Trajectory of the stripped electrons was also investigated even if they turned back to the upstream direction.
- These investigations are still going on.

REFERENCES

[1] M. J. Shirkata et al., Proc. EPAC'04, July 2004, Lucerne(2658-2660), <http://accelconf.web.cern.ch/AccelConf/e04/PAPERS/THPLT071.PDF>

[2] M. J. Shirkata et al., Proc. SAST2003, November 2003, Tsukuba(389-391)

[3] M. J. Shirkata et al., Proc. EPAC'02, June 2002, Paris(1670-1672), <http://accelconf.web.cern.ch/AccelConf/e02/PAPERS/WEPRI039.pdf>

[4] M. J. Shirkata et al., to be published.